2025 7th International Conference on Energy Systems and Electrical Power (ICESEP) | 979-8-3315-9557-9/25/$31.00 ©2025 IEEE | DOI: 10.1109/ICESEP66633.2025.11155308

Combined Heat Transfer Models and Dynamic Optimization Method for High-Pressure Feedwater Heat Exchanger in Nuclear Power Plant

Hongdong Yang
SPIC LAIYANG NUCLEAR ENERGY CO.,LTD.
Laiyang,Shandong,China
Email: yanghongdong01@spic.com.cn

Xiangyu Zhu*
STATE NUCLEAR ELECTRIC POWER PLANNING DESIGN AND RESEARCH INSTITUTE CO.,LTD.
Beijing,China
* Corresponding author: zhuxiangyu@spic.com.cn

Leishuo Wang
STATE NUCLEAR ELECTRIC POWER PLANNING DESIGN AND RESEARCH INSTITUTE CO.,LTD.
Beijing,China
Email: wangleishuo@spic.com.cn

Xiangzhi Zheng
SPIC LAIYANG NUCLEAR ENERGY CO.,LTD.
Laiyang,Shandong,China
Email: zhengxiangzhi@spic.com.cn

***Abstract*—In order to establish numerical heat transfer models suitable for high-pressure heaters in nuclear power units and improve calculation accuracy,four heat transfer calculation theories were introduced:the Dittus-Boelter model,Gnielinski model,Shell-side single phase model,and Shell-side horizontal tube condensation model.Four combined models based on different theories were applied to verify the design parameters of a high-pressure feedwater heater under various load conditions.The results indicated that the differences in heat transfer calculations among these model combinations were relatively minor,with a maximum deviation of 3.8% being observed compared to the designed heat transfer capacity of the heater.Through optimization of the established model combinations by the introduction of a dynamic correction coefficient, the maximum deviation of calculated heat transfer was reduced to 0.55%,demonstrating significant improvement in accuracy.**

Keywords-heat transfer coefficient; high-pressure heat exchanger; combined heat transfer model

I. Introduction

Shell-and-tube heat exchangers are widely used in thermal and nuclear power plants, due to their low manufacturing cost and high suitability for high-temperature and high-pressure conditions [1]. This kind of heat exchanger is commonly employed as the primary heat exchange equipment in high-pressure feedwater systems of nuclear power plants[2–4]. For example, shell-and-tube heat exchangers with high-pressure can exhaust steam from the steam turbine, and the steam enters the shell side to heat the feedwater inside the tubes, to improve thermal efficiency[5]. However, the internal structure of high-pressure heat exchanger is complex, containing the tube bundle, tube sheet, and shell. The tube sheet and shell have interactions with other components during the operation, and parameters like tube arrangement and tube diameter can affect thermal efficiency. Besides, the the working medium has multiple phases, and the fluid path is circuitous. The fluid velocity varies greatly in different areas and is affected by cross-sectional area of the shell and the obstruction coefficient of components. Due to these complex characteristics of the internal structural and fluid flow, the coefficient calculation of the heat transfer need to consider many variables and their relationships, increasing the calculation difficulty[6]. Therefore various numerical models have been developed based on theoretical analysis and engineering experience to simplify the calculation methods of the heat transfer coefficients [6–8].

The shell-side heat transfer form for high-pressure feedwater heat exchanger is convective heat transfer between the steam and the outer wall of the tubes [9]. Common empirical models include the shell-side single-phase heat transfer model and the horizontal tube condensation model (including condensate film) [10–12]. The tube-side heat transfer form is convective heat transfer between feedwater and the inner tube wall, with theoretical models such as the Dittus-Boelter model and the Gnielinski model [13].

In this paper, heat transfer models have been established for a high-pressure feedwater heat exchanger in the secondary circuit of a nuclear power plant. Four kinds of combined heat transfer models for tube-side and shell-side have been used to verify the design heat transfer coefficient under different loads. The differences between the calculation results in four combined models and the design value have been analyzed.

Based on the combined models, a dynamic optimization method has been proposed. Dynamic correction coefficients based on the operational conditions have been introduced, which can reflect the real variations of the thermal parameters for the high-pressure heat exchanger.

II. Heat Transfer Model of the Heat Exchanger

A. Basic Physical Model

The shell-and-tube heat exchanger is a kind of surface heat exchangers, where heat is primarily transferred through heat convection between the tube walls and the fluids on both sides.

Authorized licensed use limited to: UNIVERSIDADE DE SAO PAULO. Downloaded on July 08,2026 at 21:35:44 UTC from IEEE Xplore. Restrictions apply.

In the physical model, the tube-side fluid flows inside the tubes, while the shell-side fluid flows out the tube bundle within the shell. Heat is transferred from the high-temperature fluid side to the other side through the tube walls. Convective heat transfer occurs between the tube-side/shell-side fluids and the tube walls, influenced by fluid velocity and physical properties (e.g., specific heat capacity, thermal conductivity). Besides, the thermal conductivity of the tube walls plays a critical role in heat transfer. The heat transfer efficiency is affected by the interactions among these factors. The basic physical model can be described by Newton's law of cooling:

$$Q = hA\ （T_s - T_f）\tag{1}$$

where:Q is the total heat transfer rate;

T_f is the fluid static temperature [K];

T_s is the tube wall surface temperature [K];

h is the overall heat transfer coefficient [W/K], obtain from Equation (2).

$$h = \frac{1}{\frac{1}{\eta_f \lambda A_s} + \frac{R_F}{\eta_f A_s}}\tag{2}$$

where: R_F is the fouling resistance coefficient[m^2K/W];

λ is the convective heat transfer coefficient of the tube wall [W/m^2K];

A_s is the heat transfer area [m^2];

η_f is the fin efficiency, range 0–1.

Assuming the fouling resistance coefficient is 0, and fin efficiency of 1, Equation (2) can be simplified to:

$$h = \lambda A_s\tag{3}$$

For a given heat exchanger, the heat transfer area A_s is fixed. Thus, the convective heat transfer coefficient, λ, directly affects the overall heat transfer coefficient, playing a significant role in the heat transfer model.

B. Dittus-Boelter Model and Gnielinski Model of the tube-side

For the tube-side, convective heat transfer occurs between feedwater (liquid phase) and the inner tube wall. Two empirical models suitable for smooth circular straight tubes, the Dittus-Boelter model and the Gnielinski model[14,15], has been established. The Dittus-Boelter model is applicable to the forced convective heat transfer for fully developed turbulent in smooth tubes, where fluid properties are constant under heating or cooling conditions. It is obtained from large amounts of experimental data and has a simple form. However Dittus-Boelter model may lack accuracy under special conditions. The Gnielinski model has a broader application range, covering both turbulent and transition fluid regimes. It performs better for complex conditions such as varying tube surface roughness, but its formula is more complex, slightly reducing calculation convenience.

Both models share the basic form:

$$\lambda = \frac{k}{D_H} \cdot Nu\tag{4}$$

where: k is the fluid thermal conductivity, [W/m.K];

D_H is the hydraulic radius (here, the tube inner diameter);

Nu is the Nusselt number.

The difference lies in the calculation of Nu. The Dittus-Boelter model calculates as:

$$Nu = \left(A + C \cdot \mathrm{Re}^m \cdot \mathrm{Pr}^n\right)\left(\frac{\mu}{\mu_w}\right)^e\left(\frac{\rho_w}{\rho}\right)^p\left(\frac{c_{p_ave}}{c_p}\right)^g \cdot \left(\frac{T}{T_w}\right)^i\left(\frac{\mathrm{Pr}}{\mathrm{Pr}_w}\right)^j\tag{5}$$

where: Re is the Reynolds number;

Pr is the Prandtl number;

μ is the fluid dynamic viscosity;

ρ is the fluid density;

C_p is the fluid specific heat,

C_{p_ave} is the average specific heat;

T is the fluid temperature;

Subscript w denotes properties at the tube wall;

A,C,m,n,e,p,g,i,j are the model coefficients.

For the Dittus-Boelter model of the tube-side in the high-pressure heat exchaner, the coefficients are set as shown in table 1:

TABLE I. COEFFICIENT VALUES FOR THE DITTUS-BOELTER MODEL

Coefficient	Value
A	0
C	0.023
m	0.8
n	0.4 (heating)[16]
e	0
p	0
g	0
i	0.5 (liquid heating)[16]
j	0

With these coefficients from table 1, Equation (5) simplifies to:

$$Nu = 0.023 \cdot \mathrm{Re}_f^{\,0.8} \cdot \mathrm{Pr}_f^{\,0.3}\left(\frac{T}{T_w}\right)^{0.5}\tag{6}$$

The Gnielinski model calculates Nu as:

Authorized licensed use limited to: UNIVERSIDADE DE SAO PAULO. Downloaded on July 08,2026 at 21:35:44 UTC from IEEE Xplore. Restrictions apply.

$$Nu = C'\left(\frac{\frac{f}{8}(\mathrm{Re}-1000)\mathrm{Pr}}{1+12.7(\frac{f}{8})^{0.5}\left(\mathrm{Pr}^{\frac{2}{3}}-1\right)}\right)\left(\frac{\mu}{\mu_w}\right)^{e'}\left(\frac{\rho_w}{\rho}\right)^{p'}\cdot \left(\frac{c_{p\,avg}}{c_p}\right)^{g'}\left(\frac{T}{T_w}\right)^{i'}\left(\frac{\mathrm{Pr}}{\mathrm{Pr}_w}\right)^{j'} \quad (7)$$

where: f is the wall friction factor;

C', e', p', g', i', j' are the model coefficients.

For the Gnielinski model of the tube-side in the high-pressure heat exchaner, the coefficients are set as shown in table 2.

TABLE II. COEFFICIENT VALUE OF THE GNIELINSKI MODEL

Coefficient	Value
C'	1
e'	0
p'	0
g'	0
i'	0.5 (liquid heating)
j'	0

With these coefficients from table 2, Equation (7) simplifies to:

$$Nu = C'\left(\frac{\frac{f}{8}(\mathrm{Re}-1000)\mathrm{Pr}}{1+12.7(\frac{f}{8})^{0.5}\left(\mathrm{Pr}^{\frac{2}{3}}-1\right)}\right)\left(\frac{T}{T_w}\right)^{0.5} \quad (8)$$

C. Single-Phase Heat Transfer Model and Horizontal Tube Condensation Model of the Shell-Side

The shell-side single phase heat transfer model, proposed by Griminson, assumes that the fluid on the shell side is in a single-phase state during heat transfer with the outer tube wall. This model has a simple form, and can provide good predictions under ideal fluid conditions with stable fluid properties. However, the accuracy of the model decreases significantly under non-ideal fluid conditions and is not applicable fot phase-change heat transfer.

Similar to the Dittus-Boelter correlation, Nu is calculated as:

$$Nu = 0.2\cdot \mathrm{Re}^{0.6}\cdot \mathrm{Pr}^{0.33}\left(\frac{\mu}{\mu_w}\right)^{0.14} \quad (9)$$

The shell-side horizontal tube condensation model assumes that condensate forms on the outer tube walls during heating, or in other word, a laminar liquid film forms between horizontal tubes. This model offers high accuracy for the condensation of horizontal tubes, but is affected by the layout of the horizontal pipes, pipe diameter, and physical properties of the condensing fluid.

For a single horizontal tube with laminar film condensation,the convective heat transfer coefficient h is calculated as:

$$h = 0.728\left[\frac{\rho_L(\rho_L-\rho_G)gh'_{LG}k_L^{\ 3}}{d_0\mu_L(T_{sat}-T_w)}\right]^{1/4} \quad (10)$$

where:g is the gravitational acceleration;

T_{sat} is the aturation temperature;

Subscript w denotes properties at the tube wall;

Subscript L is the liquid phase;

Subscript G is the gas phase.

D. Modeling of Heat Transfer

Based on the heat transfer theories presented above, four distinct modeling combinations were established for the shell-and-tube heat transfer analysis, as detailed in Table 3.

TABLE III. COMBINED MODELS FOR HEAT TRANSFER

Combination	Tube-Side Model	Shell-Side Model
Group 1	Dittus-Boelter	Single-phase
Group 2	Gnielinski	Single-phase
Group 3	Dittus-Boelter	Horizontal tube condensation
Group 4	Gnielinski	Horizontal tube condensation

The design flow rates of the high-pressure heater under various load conditions are presented in Table 4, where the 100% MCR condition corresponds to the unit's rated full-load power output, while the power levels of other operating conditions decrease proportionally.

TABLE IV. DESIGN FLOW OF HIGH-PRESSURE HEATER

Load	Shell-Side Flow (kg/h)	Tube-Side Flow (kg/h)
100%MCR	709190.5	4049244
90%MCR	619080	3588192
80%MCR	533656	3138192
75%MCR	492980.5	2917692
60%MCR	371460.5	2270304
50%MCR	282886.5	1853424
30%MCR	129543	960336

The design parameters of the heat transfer for the shell-side and tube-side under various loads are provided in Table 5 and Table 6.

TABLE V. DESIGN PARAMETERS OF HEAT TRANSFER FOR THE SHELL-SIDE

Load	Shell-Side Inlet Temperature (°C)	Shell-Side Outlet Temperature (°C)	Temperature Difference (°C)
100%MCR	210.2	189.5	20.7
90%MCR	204.5	184.7	19.8

Authorized licensed use limited to: UNIVERSIDADE DE SAO PAULO. Downloaded on July 08,2026 at 21:35:44 UTC from IEEE Xplore. Restrictions apply.

80%MCR	198.3	179.5	18.8
75%MCR	194.9	176.8	18.1
60%MCR	184.0	167.3	16.7
50%MCR	175.5	159.9	15.6
30%MCR	149.9	137.4	12.5

TABLE VI. DESIGN PARAMETERS OF HEAT TRANSFER ON THE TUBE-SIDE

Load	Tube-Side Inlet Temperature (℃)	Tube-Side Outlet Temperature (℃)	Temperature Difference (℃)
100%MCR	183.9	207.4	23.5
90%MCR	179.1	201.7	22.6
80%MCR	173.9	195.5	21.6
75%MCR	171.2	192.1	20.9
60%MCR	161.7	181.2	19.5
50%MCR	154.3	172.7	18.4
30%MCR	131.8	147.1	15.3

According to the design parameters of 75%MCR load, the tube-side and shell-side flows and specific enthalpy have been set as input, while the outlet specific enthalpy and temperature have been calculated for model verification.

III. CALCULATION RESULTS AND ANALYSIS

A. Silumation parameters

Based on the design parameters of a high-pressure feedwater heater, a one-dimensional simulation model was established using FLOWNEX software, through which the flow characteristics and heat transfer performance were comparatively analyzed under different operating conditions with various heat transfer model combinations.The simulation parameters are as follows:

The high-pressure heater is equipped with a total of 3,971 heat exchange tubes, each measuring 15.88 mm in outer diameter with a wall thickness of 1.507 mm, configured in a two-pass arrangement with ten baffles installed on the shell side.All model combinations maintain identical internal structural parameters of the heater.

For the boundary conditions, the shell-side inlet medium was defined as high-temperature steam with a mass-flow inlet boundary, where the flow rates were referenced from Table 4 and the temperatures from Table 5. The tube-side inlet medium was specified as liquid water, also modeled as a mass-flow inlet boundary, with flow rates obtained from Table 4 and temperatures from Table 6. Both the tube-side and shell-side outlets were set as pressure boundaries based on the operating pressures of their respective downstream pipelines under corresponding working conditions.

The two-phase flow characteristics of both water and steam were calculated using the IAPWS-F97 standard for thermodynamic property evaluation.All models assumed zero fouling resistance ($R_F = 0$) and 100% fin efficiency ($\eta_f = 1$) across all operating scenarios.

B. Flow Characteristics Analysis

In the range from 100%MCR load to 30%MCR load, Reynolds number of the shell-side has been calculated, as shown in Figure 1. Reynolds number of the tube-side are shown in Figure 2. The following observations can be made from these figures:

As the load decreases, the steam flow at the in let of the shell-side decreases, and the Reynolds number of the shell-side shows a decreasing trend, but the fluid state remains turbulent.

1) At 100%MCR and 90%MCR loads, fluid velocity of the shell-side is relatively high, and the values of Re for the horizontal tube condensation model and the single-phase heat transfer model show no significant difference. After the load decreases, the difference of Re increases, with the maximum difference of 16.01% (at 30% MCR load).

2) The trend of Re change on the tube-side is consistent with that on the shell-side. However, due to the different fluid states, the Re value on the tube side is much larger than that on the shell side. Moreover, the difference of Re valus among the various combinations on the tube side range from 0.8% to 1.52%.

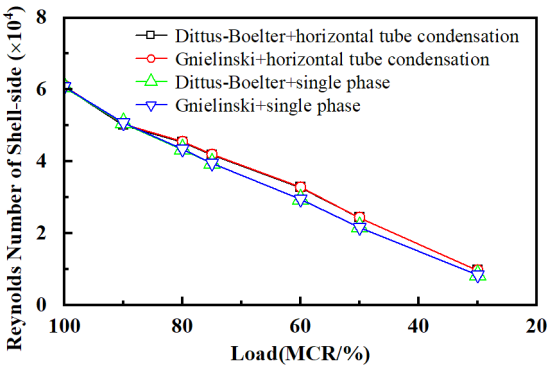

Figure 1. Reynolds Number of the shell-side

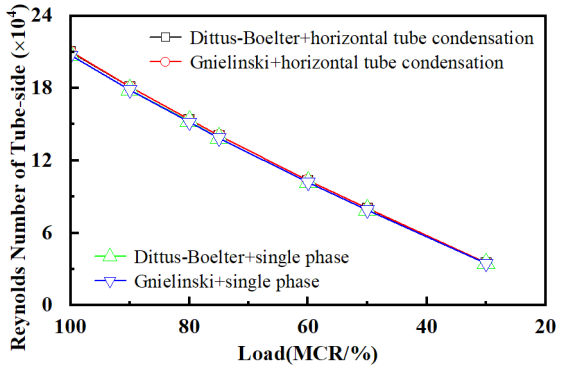

Figure 2. Reynolds Number of the tube-side

C. Characteristic Analysis of Heat Transfer

The Nusselt number (Nu) is selected as the characteristic parameter to analyze the heat transfer performance. Based on the horizontal tube condensation model, the convective heat transfer coefficient can be calculated directly, and Nu values on the shell-side can not be obtained. Therefore, the Nusselt number on the tube-side has been mainly analyzed. Figure 3

Authorized licensed use limited to: UNIVERSIDADE DE SAO PAULO. Downloaded on July 08,2026 at 21:35:44 UTC from IEEE Xplore. Restrictions apply.

shows the average Nu values of the combined models on the tube-side under different load conditions. It can be found that the Nu values have the same variation trend as Re values. The Nu values from the Dittus-Boelter model are always lower than those form the Gnielinski model. However, as the load decreases, the difference between the Nu values gradually decreases.

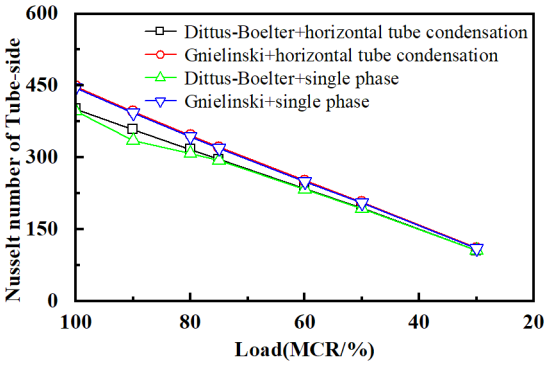

Figure 3. Nusselt Number on the tube-side

D. *Temperature Feature Analysis*

As the result of heat transfer among different combined models for the high-pressure heat exchanger, temperature can directly reflect the difference between the calculated heat transfer effect and the design heat transfer effect. Figure 4 and 5 show the outlet temperature difference of the combined models on the shell-side and tube-side, under 30%MCR to 100%MCR loads. It can be found that:

1) The outlet temperatures on both the shell-side and tube-side change in the same trend with different loads. At 75% load, the outlet temperature of four combined models are closest to the design temperatures.

2) At the low loads, the outlet temperature of the combined models on the shell-side is lower than the design value, with the maximum difference of 4.17℃ to 4.2℃ at 30%MCR load. As the load increases, the outlet temperature is higher than the design value, with the maximum difference of 2.4℃ to 2.68℃ at 100%MCR load. Due to the relatively stable state of the fluid on the tube side and the large flow, the difference in heat transfer has little influence on the temperature. Therefore, compared to the shell side, the absolute temperature difference is smaller on the tube side.

3) The heat transfer has been calculated based on the change in fluid specific enthalpy. The design value of specific enthalpy at the inlet and outlet on the shell-side is 481.9 kJ/kg at 30%MCR load. The calculation value is changed from 499.7 kJ/kg to 500.1 kJ/kg, with the maximum difference 3.8% from the design value of the heat transfer.

4) From the calculation differences among the combined models, at high loads (≥75%MCR load), the combined model of Dittus-Boelter and horizontal tube condensation is closer to the designe value, while at low loads (<75%MCR load), the combined model of Dittus-Boelter and single-phase is closer to the design value.

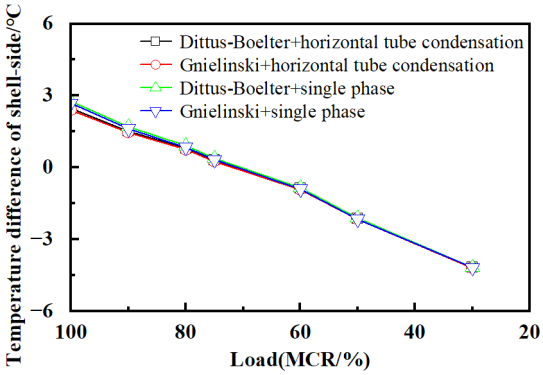

Figure 4. Outlet temperature differece between the combined models and the design value on the shell-side

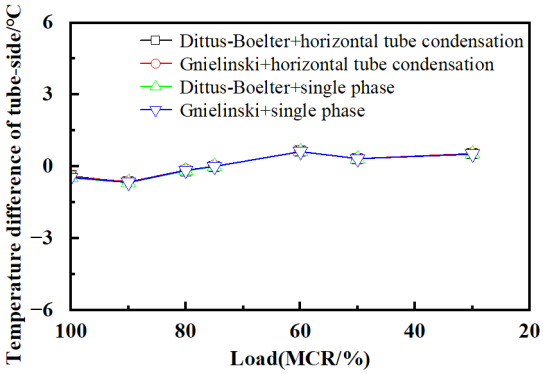

Figure 5. Outlet temperature differece between the combined models and the design value on the tube-side

E. *Model Optimization*

Above analysis reveals that the calculation difference among the four combined heat transfer models is negligible, and variation trends of the models are consistent with the design value. However, difference of 3.8% exists between the calculation values and design values of the heat transfer. The difference may be affected by the combined effects of multiple complex factors, such as the structural characteristics of internal components, and the dynamic changes of fluid flow. These factors make it difficult for the combined models to reflect the actual heat transfer situation accurately. In order to reduce the difference, the combined models have been optimized by introducing a dynamical correction coefficient ε, as shown in Equation (11). The correction coefficient can significantly reduce difference according to the actual heat transfer situation.

$$\lambda = \varepsilon\ (Q_{flow}) \cdot \frac{k}{D_H} \cdot Nu \tag{11}$$

Taking the Dittus-Boelter and Single phase model combination as an example, the applicable correction coefficients under various load conditions were dynamically invoked. The total tube-side mass flow rate, Q_{flow}, was adopted as the key variable representing unit load, establishing a linear functional relationship between ε and unit load. Identical correction coefficients were applied to both tube-side and shell-side to ensure the combined model maintained solution

Authorized licensed use limited to: UNIVERSIDADE DE SAO PAULO. Downloaded on July 08,2026 at 21:35:44 UTC from IEEE Xplore. Restrictions apply.

accuracy across different load conditions. Through debugging, the determined values of dynamic correction coefficients are presented in Table 7.

TABLE VII. VALUES OF DYNAMIC CORRECTION COEFFICIENT

Unit Load	Tube-Side Flow (kg/h)	Correction Coefficient ε
100%MCR	4049244	2.16
90%MCR	3588192	1.67
80%MCR	3138192	1.17
75%MCR	2917692	1
60%MCR	2270304	0.7
50%MCR	1853424	0.6
30%MCR	960336	0.35

The calculation results of the optimized model are illustrated in Figure 6. The maximum difference between the combined model and the design temperature of the outlet on the shell-side is reduced to 0.7°C, while the maximum difference on the tube-side is reduced to 0.4°C. Difference rate in heat transfer of the optimized model is reduced to 0.55%, compared to the original combined model. It can be found that the optimized combined model meets the accuracy requirements for the high-pressure heat exchanger. The dynamical correction coefficient proposed in this study is applicable for the in heat transfer model.

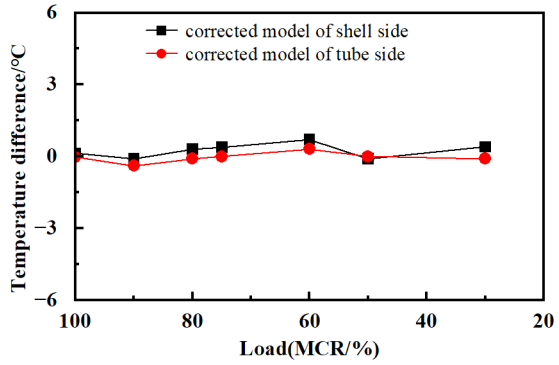

Figure 6. Difference between corrected models and design values

IV. CONCLUSION

In this paper, four numerical heat transfer theories have been introduced and four combined models have been established by FLOWNEX. Calculation results of each combined model have been compared and analyzed. Following conclusions are obtained:

1) *Nu* values of the tube-side calculated by the Dittus-Boelter model are lower than those from the Gnielinski model, but the difference decreases at lower loads.

2) Above 75%MCR load, calculation results from the Dittus-Boelter and horizontal tube condensation model is more closer to the design values. Below 75%MCR load, the Dittus-Boelter and single-phase model has better consistency with the design values. Four combined models have a maximum difference of 3.8% from the design value.

3) The combined models have been optimized by a dynamical correction coefficient. Compared with the combined models before optimization, the maximum difference is reduced to 0.55%.

4) In subsequent researches, the numerical model and method proposed in this paper is expected to be refined and enhanced to expand their applicability to a wider range of scenarios.For example, the simulation of the transient thermodynamic properties of a system during rapid load changes;Or for the implementation of an integrated 1D-3D coupled simulation framework.

REFERENCES

[1] Xu Q, Jiang Y F. Numerical simulation of the superheat section in feedwater heaters [J]. Energy Engineering, 2022, 42(03): 18–22.

[2] Patankar S V, Spalding D B. Heat exchangers: Design and theory sourcebook [J]. 1974.

[3] Habib M A, Attya A E, Mceligot D M. Calculation of Turbulent Flow and Heat Transfer in Channels With Streamwise-Periodic Flow [J]. Journal of Turbomachinery, 1988, 110(3): 405–411.

[4] Prithiviraj M, Andrews M J. Three dimensional numerical simulation of shell-and-tube heat exchangers. part i: foundation and fluid mechanics [J]. 1998, 33(8): 799–816.

[5] .Qian H, Wang H, Zhang D. Study on Heat Transfer Coefficient of High-pressure Heater based on DA-DBSCAN [J]. Thermal Power Engineering, 2024, 39(03): 100–108.

[6] Sun C,Ai S Q,Liu Y C.Numerical simulation plate side flow heat transfer new plate-shell heat exchanger with considering physical property changes and shell heat transfer[J].Chemical Industry and Engineering Progress,2024,43(4):1676-1689

[7] Liang X Z,Huang Z Y,Ai F M et al. Dynamic model by transfer function and parameter determination method of plate fin heat exchanger.Journal of Beijing University of Aeronautics and Astronautics [J] , 2024, 50(1):154-162.

[8] Zou Z. CANDU-6 Nuclear Power Plant Systems and Operation: Conventional Island Systems (I) [M]. Beijing: Atomic Energy Press, 2010.

[9] Wang M, Li Q, Qi D, et al. Effect of surface tension model on numerical calculation results of heat transfer in falling film flow over horizontal elliptical tubes [J]. Heating Ventilating & Air Conditioning, 2024, 54(05): 109–116.

[10] Ophir A, Lokiec F. Advanced MED process for most economical sea water desalination [J]. Desalination, 2005(1/3): 182.

[11] Zhao C Y, Zheng C M, Wang X S, et al. Correlations of falling film hydrodynamics and heat transfer on horizontal tubes: A review [J]. 2024.

[12] Zhao C Y, Qi D, Ji W T, et al. A comprehensive review on computational studies of falling film hydrodynamics and heat transfer on the horizontal tube and tube bundle [J]. Applied Thermal Engineering, 2022: 202.

[13] Tao W. Heat Transfer [M]. Xi'an: Northwestern Polytechnical University Press, 2006: 219–221.

[14] WANG Jianfei, SONG Guanqiang, ZHAO Guanjia. Experimental study on heat transfer characteristics of flue gas condenser[J]. Boiler Technology, 2023, 54(1): 9−14.

[15] Lu J, Ren K, Tang J, et al. Numerical simulations of laminar film condensation of H2O/air or H2O/CO2 on a vertical plate[J]. Heat Transfer Engineering, 2023, 44(8): 720–733.

[16] NIE Xin, XIE Haiyan, LIU Hui, et al. A simulated study of convective-condensation heat transfer of saturated wet gas[J]. Journal of Central South University(Science and Technology), 2024, 55(12): 4675−4686.

Authorized licensed use limited to: UNIVERSIDADE DE SAO PAULO. Downloaded on July 08,2026 at 21:35:44 UTC from IEEE Xplore. Restrictions apply.